Published in final edited form as:
J Neurosci Methods. 2011 November 15; 202(2): 199–208. doi:10.1016/j.jneumeth.2011.08.020.

Tonic and Phasic Release of Glutamate and Acetylcholine Neurotransmission in Sub-regions of the Rat Prefrontal Cortex Using Enzyme-based Microelectrode Arrays

Catherine E. Mattinson[a,b], **Jason J. Burmeister**[b], **Jorge E. Quintero**[a,b], **Francois Pomerleau**[a,b], **Peter Huettl**[a,b], and **Greg A. Gerhardt**[a,b]

Catherine E. Mattinson: cmattinson@uky.edu; Jason J. Burmeister: Jasonburmeister@yahoo.com; Jorge E. Quintero: Jequin0@email.uky.edu; Francois Pomerleau: Fpome2@email.uky.edu; Peter Huettl: Pfhuet2@email.uky.edu

[a]Department of Anatomy and Neurobiology, Morris K. Udall Parkinson's Disease Research Center of Excellence

[b]Center for Microelectrode Technology, University of Kentucky, 306 Davis Mills Building, 800 Rose St., Lexington, KY 40536-0098, USA

1. Introduction

The medial prefrontal cortex (mPFC) is an area of the brain that is critically involved in higher cognitive processes such as learning, memory, and attention. Glutamate and acetylcholine (ACh) in combination with monoamine neurotransmitters (Berger et al., 1976; Brown et al., 1979; de Brabander et al., 1993; Gratton et al., 1989; Perry et al., 2011; Thierry et al., 1983) are essential for prefrontal cortical functioning. The mPFC receives glutamatergic inputs from the thalamus (Gigg et al., 1992; Leonard, 1969; Pirot et al., 1994), basal forebrain (Henny and Jones, 2008), hippocampus (Gigg et al., 1994; Jay et al., 1992), and amygdala (McDonald, 1996). This brain area also receives acetylcholine input from the basal forebrain as part of the basal forebrain cortical cholinergic system (Mesulam et al., 1983). The loss or antagonism of these specific glutamatergic and acetylcholinergic afferents has been shown to result in deficits in spatial working memory (Bailey and Mair, 2005; Romanides et al., 1999), passive avoidance tasks (Torres et al., 1994), and attention (McGaughy et al., 1996), highlighting the importance of these neurotransmitter systems in daily cognitive functioning. Dysregulation of the glutamatergic and/or acetylcholinergic circuitry in the mPFC has been implicated in disorders such as schizophrenia (Bauer et al., 2008; Benes et al., 1992; Crook et al., 2001; Olbrich et al., 2008; Oni-Orisan et al., 2008; Sarter et al., 2005; Tsai et al., 1995; Woo et al., 2008; Zmarowski et al., 2009), Alzheimer's disease (Burbaeva et al., 2005; Francis et al., 1999; Kashani et al., 2008; Perry et al., 2011; Trabace et al., 2007), and drug addiction (Arnold et al., 2003; Lu et al., 1999; McFarland et al., 2003; Sofuoglu and Mooney, 2009; Williams and Steketee, 2004). The overlap and possible interactions of these two neurotransmitter systems underscores the importance of understanding both the tonic and phasic aspects of glutamate and ACh neurochemical signaling in the mPFC and could lead to a better understanding of alterations associated with neuropathologies.

Until recently, microdialysis was unchallenged as the gold standard technique for measuring *in vivo* levels of neurotransmitters in the mammalian central nervous system, and the majority of what is known about mPFC glutamate and ACh levels comes from microdialysis

Corresponding author: Dr. Greg A. Gerhardt, 306 Davis Mills Building, 800 Rose Street, Lexington, KY40536-0098, Phone: 859-323-4531, Fax: 859-257-5310, gregg@uky.edu.

studies. However, microdialysis is limited in two critical areas 1) by its temporal resolution (minutes) (Nandi and Lunte, 2009) and 2) by its spatial resolution (millimeters) (Clapp-Lilly et al., 1999). Furthermore it has been shown to cause extensive brain damage (millimeters) around the probe (Clapp-Lilly et al., 1999; Georgieva et al., 1993; Grabb et al., 1998).

Our group has worked extensively on a microelectrode array (MEA) technology that allows for measurements of neurotransmitter synaptic spillover at rates of 1-4 Hz. With platinum recording sites having a small footprint (15 × 333 μm) and measuring neurotransmitters in the nanomolar range, the MEAs allow for the characterization of specific brain subregions, such as those in the prefrontal cortex (Bruno et al., 2006; Burmeister et al., 2008; Day et al., 2006; Nickell et al., 2005; Stephens et al., 2009). mPFC subregions including the cingulate cortex (Cg1), prelimbic cortex (PrL) and infralimbic cortex (IL) are measured on the scale of microns and are readily measured with the MEA technology.

In this paper, we report experiments that used our MEA technology to gain insight into potential subregional differences in tonic and phasic release of glutamate and ACh in the rat mPFC. We first measured resting neurotransmitter levels within the Cg1, PrL, and IL of the mPFC. Secondly, we examined the dynamics of KCl-evoked release of glutamate and ACh in the Cg1, PrL and IL to investigate additional transient or phasic release of these neurotransmitters. These experiments provide new information regarding the regional signaling properties of glutamate and ACh in different subregions of the mPFC, an area of the brain that is implicated in many neuropathologies.

2. Materials and Methods

2.1 Animals

Male Fischer 344 rats (Harlan, Indianapolis, IN), aged 3 – 6 months, were used for all experiments (n = 17). Animals were individually housed and maintained on a 12 h light: 12 h dark cycle (lights on at 06:00 h). Animals had access to food and water *ad libitum* and were monitored by the Department of Laboratory Animal Resources at the University of Kentucky. All protocols used in the experiments were approved by the Institutional Animal Care and Use Committee.

2.2 Microelectrode Arrays

Ceramic based conformal MEAs were made sensitive to and selective for glutamate or ACh detection using enzyme layers coated onto the surface of platinum (Pt) recording sites (Figure 1A) (Burmeister et al., 2008; Day et al., 2006). The MEAs used for these studies were the S2 configuration with Pt recording sites, each measuring 15 × 333 μm and arranged in two pairs, with 100 μm separating the pairs. Before coating, MEAs were prescreened through cleaning and preliminary testing to minimize inherent Pt site differences (MEAs that did not meet criteria were not used for experiments). Glutamate detecting MEAs were coated with a solution of 0.1 units/μL glutamate oxidase, 1% BSA, and 0.125% glutaraldehyde on one pair of Pt recording sites, while the second pair of recording sites was coated with only the BSA/glutaraldehyde coating matrix solution and allowed to cure a minimum of 48 hours before use (Figure 1A). As glutamate is not inherently electroactive, the glutamate oxidase enzyme was used to catalyze the oxidation of glutamate to α-ketoglutarate and H_2O_2, an electroactive reporter molecule. To enhance selectivity a size exclusion layer of m-Phenylenediamine (mPD) was electrodeposited on to the Pt recording sites prior to calibration. The mPD layer greatly reduces electroactive interferents from coming into contact with all recording sites. The signal from the pair of recording sites with only the coating matrix was subtracted from the signal produced by the glutamate oxidase-coated sites to allow for a self-referencing signal subtraction technique

(Burmeister and Gerhardt, 2001; Burmeister et al., 2008; Burmeister et al., 2002; Day et al., 2006).

MEAs configured for ACh detection (Figure 1B) required a dual enzyme coating scheme to produce the H_2O_2 reporter molecule, as ACh is also non-electroactive. Acetylcholinesterase was used to hydrolyze ACh into acetate and choline, and then choline was catalytically oxidized by choline oxidase to produce H_2O_2 (Bruno et al., 2006). MEAs were coated with a solution of 0.2 units/μl choline oxidase, 0.9% BSA and 0.11% glutaraldehyde on all four sites and allowed to cure at 4°C for a minimum of 48 hours. MEAs were then coated with 0.83 units/μl human recombinant acetylcholinesterase, 0.83% BSA, and 0.10% glutaraldehyde on one pair of sites, and the BSA/glutaraldehyde solution on the other pair of sites to ensure comparable coating thickness between the pairs of sites and to allow for self-referencing (Burmeister et al., 2008). Again, in order to enhance selectivity a size exclusion layer of mPD was electrodeposited on to the Pt recording sites prior to calibration. Each of the MEA sites were tested to determine selectivity vs. dopamine during an *in vitro* calibration to ensure that the mPD electrodeposited onto sites was uniform. The signal from the choline oxidase-coated sites was subtracted from the combined acetylcholinesterase/choline oxidase sites to determine the self-referenced ACh signal.

Glutamate and ACh were recorded with a FAST16mkII instrument (Quanteon L.L.C., Nicholasville, KY). Detection was achieved by amperometric measurements using a potential of +0.7 V vs. an Ag/AgCl electrode, which detected H_2O_2 that was oxidized at the surface of the Pt recording sites; the electrons from the oxidation reaction produced a signal that was recorded and digitized by the FAST16mkII system. All recordings were performed at a final output frequency of 1 Hz. Before each experiment, MEAs were calibrated *in vitro* using stepwise additions to increase concentrations of glutamate or ACh, as well as, electroactive interferents as previously described (Burmeister and Gerhardt, 2001; Burmeister et al., 2002). Sensitivity, linearity, limit of detection, and selectivity over electroactive interferents were calculated for all MEAs using the *in vitro* calibration data prior to experimentation. MEAs used in glutamate experiments had an average slope of -4.2 ± 2.0 pA/μM, an average limit of detection of 0.99 ± 0.9 μM, a linearity $R^2 > 0.99$, and an average selectivity of 57:1 ± 37. In ACh experiments, MEAs averaged a slope of -5.8 ± 2.6 pA/μM, a limit of detection of 0.30 ± 0.44 μM, a linearity $R^2 > 0.99$, and a selectivity of 415:1 ± 716.

A micropipette (10 μm internal diameter) for exogenous KCl- delivery (see below) was affixed to the MEA using sticky wax (Kerr Corp., Orange, CA). The tip of the micropipette was centered among all four recording sites approximately 75 μm away from the surface of the MEA, allowing for solution delivery during *in vivo* recordings.

2.3 In Vivo Recordings

In vivo glutamate and ACh recordings were performed as previously described (Burmeister et al., 2008; Day et al., 2006). Briefly, rats were anesthetized with urethane i.p. (1.25-1.5 g/kg). After the animal was secured in a stereotaxic frame, a craniotomy was performed over the placement site of interest and the dura removed. A hole was also drilled contralateral to the placement for a miniature Ag/AgCl reference electrode. The micropipette attached to the MEA was filled with an isotonic KCl solution (70 mM KCl, 79 mM NaCl, 2.5 mM $CaCl_2 \cdot 2H_2O$; pH = 7.4) and connected to a Picospritzer III (Parker Hannifin Corp, NJ) to allow for local applications of KCl into the extracellular space. The MEA/micropipette assembly was lowered into the mPFC (AP: +3.2 mm; ML: ±0.8 mm; DV: -1.5 to -5 mm; from bregma (Paxinos and Watson, 2004) using a Narishige MO-10 microdrive (Figure 2A). The MEA assembly was lowered in 0.5 mm increments and recordings were taken at each depth to record glutamate or ACh levels along the dorsal-ventral axis of the mPFC. Once lowered

into place, basal levels were established over ten minute recording durations, and then KCl solution was ejected (75-100 nl) to evoke glutamate or ACh signals: volume of KCl delivered was monitored using a microscope fitted with a calibrated reticule (Friedemann and Gerhardt, 1992). At the end of the experiment, animals were euthanized and histology was performed to confirm MEA placement. Only data collected from confirmed electrode placements in the different subregions of the mPFC were included in the final data analysis; data from two animals were excluded in these studies.

2.4 Data Analysis

Collected data were processed using a custom Matlab®-based analysis package. Data parameters analyzed were resting (tonic release) neurotransmitter levels (average of the ten data points prior to the first ejection at each depth) and data from potassium-evoked release (phasic release) of glutamate or ACh that included: peak amplitude, T_{80} (time for 80% of the signal to decay to baseline), and k_{-1}, best fit line of first order rate constant of the signal return to baseline (Figure 2B). Glutamate and ACh KCl-evoked peaks were volume matched (75-100 nL) for data analysis. Outliers were eliminated from data using a Grubb's test before analyses were conducted. As data was not always attainable at every depth throughout the depth profile due to clogging of the tips of the micropipettes, occasional data drop out occurred. Thus, a one-way ANOVA with a Bonferroni *post hoc* test was used to analyze the potassium evoked data and resting levels between glutamate and ACh were analyzed using a two-way ANOVA. Correlations were also performed to compare the log of KCl-evoked data and resting data for each neurotransmitter. Significance was defined as $p < 0.05$.

3. Results

3.1 Glutamate and acetylcholine resting levels are stable across subregions

Glutamate and ACh recordings in the mPFC focused on three subregions: the Cg1, PrL, and IL. For both neurotransmitters, resting levels were calculated using the self-referenced signals (Figure 2B). When average resting levels of glutamate were compared among brain regions (Figure 3A), they were found to be similar ($F(2,18) = 0.069$; $p = 0.93$), with only a 0.7 μM difference between the highest and lowest levels. Interestingly, analyses of average ACh resting levels revealed comparable resting levels (Figure 3B; $F(2,17) = 0.47$; $p = 0.63$) of 0.6 – 1.0 μM for the Cg1, PrL and IL. There was a significant main effect between the two neurotransmitters ($F(1,35) = 16$; $p = 0.0003$), however, the resting levels of glutamate and ACh were not significantly different within subregions of the mPFC.

3.2 KCl-evoked glutamate release is similar among subregions in the mPFC

KCl-evoked release of glutamate was successfully carried out in the Cg1, PrL and IL subregions of the mPFC. Local application of KCl was seen to produce detectable and transient increases in extracellular glutamate that lasted for, on average, 3-5 seconds. Representative tracings of KCl-induced glutamate release from each brain region were compared (Figure 4A) to illustrate the similar peak amplitudes among the subregions of the mPFC. The tracings indicate the uniformity among signals, with similar peak rise times, peak amplitudes, and similar decay profiles.

The glutamate peak amplitudes, T_{80} values, and k_{-1} values were used to characterize KCl-evoked release of glutamate (see Figure 2B). Measures of glutamate release revealed no significant differences in the peak amplitudes of glutamate (Figure 4B; $F(2,15) = 1.8$; $p = 0.21$) or T_{80} values (Table I; $F(2,16) = 1.9$; $p = 0.18$) in the different subregions. Glutamate k_{-1} values were also comparable among brain regions (Table I; k_{-1}: $F(2,16) = 0.31$; $p = 0.74$). Correlations of the log of KCl-evoked release of glutamate with resting levels of

glutamate were not significant for any subregion of the mPFC (Figure 7A, B, C; Cg1, p = 0.97; PrL, p = 0.12; IL, p = 0.20).

3.3 Acetylcholine signaling parameters are similar among brain regions

Studies were carried out to investigate KCl-evoked release of ACh in the subregions of the mPFC. Similar to the glutamate studies, KCl was seen to produce detectable and transient release of ACh lasting 5-10 seconds in the mPFC. The similarity among ACh release and uptake from each brain subregion are further illustrated in Figure 5A. KCl-evoked ACh peaks rose to peak amplitudes in a similar manner, and decayed at similar rates, resulting in comparable signaling parameters among the Cg1, PrL, and IL. When ACh signaling parameters were compared among the three brain subregions, no significant differences were found suggesting homogeneity of ACh neurotransmission in the mPFC. Peak amplitudes showed uniformity, (Figure 5B; $F(2,26) = 1.1$; $p = 0.35$) thus further characterizing KCl-induced ACh release among the brain subregions. When the log of KCl-evoked releases of ACh were correlated with ACh resting levels within each subregion, a significant difference in the Cg1 was found (Figure 7D; Cg1, $p = 0.049$). No significance was found in either the PrL (Figure 7E; $p = 0.93$) or the IL (Figure 7F; $p = 0.29$). ACh uptake parameters including T_{80} values were also homogeneous (Table II; $F(2,23) = 0.32$; $p = 0.73$), as were k_{-1} values (Table II; k_{-1}: $F(2,26) = 0.096$; $p = 0.91$).

3.4 Comparisons of KCl-evoked glutamate and acetylcholine reveal significant differences between the neurotransmitters

We compared the peak amplitudes of both neurotransmitters to contrast mPFC glutamate and ACh KCl-evoked release (Figure 6A). While significant differences were not found within each neurotransmitter, significant differences did exist between neurotransmitters. ACh peak amplitude measurements ranged from 5.3 – 7.1 μM, and glutamate peak amplitude concentrations measured 1.8 – 2.9 μM. Analyses revealed that the peak levels of ACh in the Cg1 were significantly higher than glutamate signals in all subregions ($F(5,41) = 5.4$; $p = 0.0007$). As compared to glutamate levels in the Cg1, Cg1 ACh levels were greater by 144%. Potassium-evoked ACh release in the Cg1 was also greater by 255% and 294% compared to glutamate levels in the PrL and IL, respectively.

We also compared T_{80} values between the two neurotransmitters, and found significant differences in decay times between glutamate and ACh ($F(5,39) = 10.6$; $p < 0.0001$). In the Cg1, ACh decay times were increased 198% as compared to glutamate decay times in the same brain subregion (Figure 6B). ACh T_{80} values in the PrL and IL were increased 189% and 330% as compared to glutamate values, respectively.

4. Discussion

These are the first studies comparing both tonic and phasic release of glutamate and ACh levels on a second-by-second time scale in individual subregions of the anesthetized rat mPFC. The results of our studies demonstrate that we can reliably measure both tonic and phasic glutamate and ACh release *in vivo* using the MEA technology. The spatial resolution of our MEAs allowed for the measurement of these neurotransmitters in discrete mPFC subregions such as the Cg1, PrL, and IL, and the sampling rate offered the ability to measure individual KCl-induced glutamate and ACh peaks. Interestingly, our data support that the glutamate and ACh neurotransmitters systems have tonic and phasic release that are uniform within the subregions, but there were significant differences in both resting and KCl-evoked release of glutamate vs. ACh in the mPFC.

4.1 Resting levels of glutamate and acetylcholine

These studies did not find significant differences in resting glutamate levels within the Cg1, PrL, and IL, although there was marked variability within each mPFC subregion. We had initially hypothesized that we would see differences among the subregions for glutamate resting levels, as glutamate is tightly regulated in the mPFC (Hascup et al., 2010). Thus, the relative homogeneity of our glutamate resting levels within the mPFC subregions was unexpected, but not unprecedented. Previous MEA work within our lab has shown that glutamate resting levels in anesthetized animals do not differ greatly between brain regions. We have reported resting glutamate levels in anesthetized rats of 1.6 ± 0.3 μM in the frontal cortex and 1.4 ± 0.2 μM in the striatum, and in the hippocampus, we have measured glutamate concentrations ranging from 2.5 μM in the CA1 region to 3.4 μM in the dentate gyrus (Stephens et al., 2009). Our glutamate resting levels of 3.7 - 4.3 μM in mPFC subregions are higher than previously reported levels from MEA studies in other brain regions, but not unreasonable. Resting levels of glutamate that have been measured using microdialysis in the mPFC have ranged from 0.23 ± 0.061 μM to 3.8 ± 0.4 μM (Del Arco et al., 1998; Ferraro et al., 2001; Hugues et al., 2007; Karreman and Moghaddam, 1996; Lupinsky et al., 2010) and 3.0 ± 0.6 μMin the striatum (Miele et al., 1996). Compared with microdialysis measures, our resting levels of glutamate are over 600% higher than previously reported microdialysis glutamate levels in the mPFC of the same strain (Selim and Bradberry, 1996). However, this difference in concentration between MEA technology and microdialysis measures can be explained because the MEAs sample the extracellular space of the brain directly rather than being separated by a membrane containing a net analyte concentration of zero driving diffusion into the microdialysis probe. Also, far less edema or gliosis occurs with MEAs than microdialysis probes, allowing for better estimates of neuronally-based release vs. release from other sources.

The Pt recording sites on the MEA only measure neurotransmitters that come into contact with the surface of the electrode (Burmeister et al., 2000). We have hypothesized that our increased glutamate resting levels and higher ACh resting levels may be the result of the enhanced spatial resolution of our MEAs that allows us to be closer to synaptic spillover, as evidenced by studies using tetrodotoxin (Day et al., 2006). Microdialysis probes may be able to pick up some spillover, but the size of the probe membranes and the inherent time constant of the microdialysis membrane (Schultz and Kennedy, 2008) is prohibitive for measuring neurochemical activity at the level of synapses (Timmerman and Westerink, 1997). Thus, the MEAs measure the concentration of the neurotransmitter that resides in the extracellular space and do not record a fractional level. Our recently reported studies support that this translated to a 5-10 fold difference of resting levels of glutamate measured by MEAs versus microdialysis in the awake animal and is largely due to the direct measurement of the neurotransmitter concentration in the extracellular space by the MEA technology (see Hascup et al., 2010).

In our first paper using MEA technology to measure ACh (Bruno et al., 2006), we did not report resting levels. However, in this set of studies we are now able to report for the first time *in vivo* resting levels of ACh using MEA technology. Similar to our glutamate hypothesis, we predicted that we would see significant differences in ACh resting levels among the subregions of the mPFC. We did not find any significant differences in resting levels of ACh among the mPFC subregions, and little variability existed within each subregion. Reported resting levels of ACh in the mPFC have widely varied from 0.58 ± 0.14 nM to 3.0 ± 0.3 μM in microdialysis studies (Arnold et al., 2001; Hernandez et al., 2008; Huang et al., 2008; Mork et al., 2009; Neigh-McCandless et al., 2002). Our ACh measurements of 0.59 – 0.96 μM fall into the higher end of the range of these previously reported microdialysis ACh concentrations. Microdialysis, with its collection times on the scale of several seconds to minutes, may allow for more ACh hydrolysis by

acetylcholinesterase, resulting in lower reported concentrations. Thus, many scientists who use microdialysis for measuring ACh levels also perfuse an acetylcholinesterase inhibitor, such as neostigmine, to prevent ACh breakdown (Nirogi et al., 2010; Ragozzino et al., 1996). However, this technique may artificially affect the measured ACh levels in the extracellular space. The detection of higher levels of both glutamate and ACh can be attributed to the improved spatial and temporal resolution of the MEA.

The present series of studies was carried out in anesthetized animals to take advantage of the brain mapping capability of the MEAs to record glutamate and ACh levels in different subregions of the mPFC in the same rat. Work from our group has shown that the administration of urethane anesthesia to awake, freely moving rats resulted in a 58% decrease in resting glutamate levels (Rutherford et al., 2007). Thus, it is likely that the anesthetic attenuated glutamate resting levels in these studies and possibly affected ACh levels as well. Even with this possible attenuation, our glutamate resting levels are still relatively high compared to microdialysis studies, but this likely relates to the aforementioned properties of the MEA measurements as compared to microdialysis. By contrast, to date we do not have any indication that urethane affects KCl-evoked release of glutamate based on our work (data not shown). Urethane has also been shown to enhance the actions of the nicotinic ACh receptor, but only to a small degree (Hara and Harris, 2002). Future studies will be carried out in the awake animal to circumvent the potential effects of anesthesia. It should also be noted that glutamate and ACh levels in the mPFC vary with rat strain. For example, glutamate levels in awake rats have been reported from 0.22 μM in Sprague-Dawley rats (Ferraro et al., 2001) to 4.2 μM in Wistar-King rats (Abekawa et al., 2000). ACh levels in rats exhibit an even greater range of resting levels, from 0.58 nM in awake Sprague-Dawley rats (Huang et al., 2008) to 3.0 μM, also in awake Sprague-Dawley rats (Mork et al., 2009). Thus, the concentrations reported in the present studies were likely affected by anesthesia and were likely dependent on the strain used.

A comparison of our resting levels of glutamate and ACh in mPFC subregions did not reveal any differences within neurotransmitters, but we did see a significant main effect between neurotransmitters, suggesting that the neurotransmitter resting levels do vary between glutamate and ACh within the mPFC. This may be due to the differential innervation of the mPFC by theses neuronal systems and/or the regulation of these neurons by other neurons and signaling molecules. Interestingly, our resting levels of ACh were extremely similar between the PrL and IL subregions, suggesting that ACh regulation is uniform in these areas. This is supported by microdialysis experiments that have sought to characterize subregions of the mPFC, and have reported similar resting levels between the prelimbic and infralimbic mPFC (Hedou et al., 2000). However, it should be noted that there was overlap between subregions due to the spatial resolution of the microdialysis technique.

4.2 Measurements of KCl-evoked release of glutamate and ACh in the rat mPFC

Although no significant differences were found in KCl-evoked glutamate release, both the peak amplitudes and the T_{80} values followed trends along the dorsal-ventral axis in the mPFC (Table I). In previous microdialysis studies that used KCl to evoke neurotransmitter release, the infusion of KCl into the mPFC resulted in an increase in glutamate levels of 90% (Frantz et al., 2002). KCl has also been reported to have no effect on glutamate levels (Welty and Shoblock, 2009). However, these studies were not specific to subregions of the mPFC, and they did not measure rapid changes in glutamate or ACh. We saw that glutamate peak amplitudes decreased ~38% from the Cg1 to the IL, while T_{80} values in the IL were also decreased by 44% as compared to T_{80} values in the Cg1. These findings are suggestive of subtle variance in the amounts of glutamate released in response to KCl, and in the time needed for 80% signal decay among mPFC brain subregions that also could relate to the extent of glutamate regulation by glutamate transporters located primarily on glia in

subregions of the mPFC (Danbolt, 2001). Additional studies are needed to further investigate this finding.

Our studies showed that potassium stimulation was seen to produce increases in extracellular ACh that ranged from ~500-1000% of the baseline or tonic ACh levels. A previous microdialysis study showed that potassium stimulation produced an increase in ACh levels of 650% (Herzog et al., 2003). Thus, the relative change from baseline or tonic ACh levels seen from potassium stimulation was in the range of that reported by microdialysis. Interestingly, our KCl-evoked ACh peak amplitude values followed a pattern similar to that of glutamate along the dorsal-ventral axis of the mPFC. Both ACh peak amplitudes and ACh uptake rates were decreased in more ventral areas as compared to dorsal areas. Our T_{80} values in the IL subregion were found to be consistent with a previous study using our ceramic based MEAs (Bruno et al., 2006).

When we compared our glutamate and ACh peak amplitudes, we found that the ACh peak amplitude concentrations were significantly higher in the Cg1 region of the mPFC (7.1 μM) than the glutamate concentrations in all subregions (1.8-2.9 μM). Acetylcholinesterase distribution in the mPFC is known to be heterogeneous (Mrzljak and Goldman-Rakic, 1992; Rajkowska et al., 1993). Thus, the varying amounts of this enzyme may be responsible for the significant ACh concentration differences. It has also been shown that the basal forebrain projects directly to the Cg1, among other areas of the mPFC (Bigl et al., 1982; Houser et al., 1985), and this may account for increased release of ACh. Additionally, the tight regulation of the glutamate signaling (Hascup et al., 2010) may result in decreased amounts of glutamate release. Our higher observed glutamate resting levels may be sufficient to maintain glutamatergic tone within the mPFC. Our studies also found significant differences in T_{80} values between glutamate and ACh within all subregions. ACh T_{80} values in the Cg1, PrL, and IL were all significantly increased as compared to glutamate T_{80} values in the same brain subregions (Figure 6B). These increased decay times seen in KCl-evoked release of ACh suggest that glutamate is being cleared more rapidly than ACh. This may be due to the separate processes that govern the breakdown of these neurotransmitters. Glutamate clearance from the extracellular space is dictated by a number of factors, including diffusion and the presence of high affinity glutamate transporters (Danbolt, 2001). Extracellular ACh is rapidly broken down by endogenous acetylcholinesterase. In addition to diffusion, choline is removed from the extracellular space via sodium dependent high affinity choline transporters (Okuda et al., 2000) and through low affinity transport (Meyer et al., 1982). Our data suggests that, based on our T_{80} values, glutamate transport may be occurring on a faster time scale than the hydrolysis of ACh and transport of choline.

For these ACh experiments, we used a human recombinant source of acetylcholinesterase in our coating solution. Many studies (Bruno et al., 2006; Giuliano et al., 2008) used acetylcholinesterase from an eel source, which became unavailable from vendors for a period of time in 2006. When the eel source of acetylcholinesterase was reintroduced, we observed that it had markedly lower unit activity than before (≥1000 units/mg of protein). This less reliable form of the enzyme was used for a number of experiments, with fairly poor results. Thus, we were forced to look for an alternative source of acetylcholinesterase. The human recombinant version of this enzyme proved to be a viable option for coating, with its higher unit activity (≥2000 units/mg of protein). We feel that the human recombinant acetylcholinesterase corrected the previous problems of measuring ACh associated with the eel source of acetylcholinesterase. The human recombinant acetylcholinesterase, as well as our curing protocol, has allowed us to optimize MEAs for *in vivo* ACh detection (Burmeister et al., 2008) and to carry out the studies described in this study.

The cholinergic system is a complex network that uses both choline and ACh for neurochemical signaling. It has been postulated that the *in vivo* hydrolysis of ACh by acetylcholinesterase occurs so rapidly (Lawler, 1961) that little ACh can escape the synaptic cleft intact, and thus measuring choline is a suitable alternative (Giuliano et al., 2008). Our data presented in this paper contradicts this hypothesis, as evidenced by our PrL resting ACh concentrations of 1.0 ± 0.7 μM, which are at least one order of magnitude higher than the levels of 0.058 – 117 nM (Brooks et al., 2007; Del Arco et al., 2007; Huang et al., 2008; Prus et al., 2007) reported in recent microdialysis studies performed in the mPFC of awake rats. The amplitudes of ACh measured from the KCl-evoked measures in this study yielded peak amplitude concentrations of 7.1 ± 3.9 μM, which were similar to those previously reported using MEA technology (Bruno et al., 2006). Even more impressive, these calculations are based on a self-referenced signal that subtracts the background current produced by the breakdown of choline. Thus, we can conclude that the subtracted signal likely reflects ACh concentrations in the mPFC, and that these ACh levels are robust enough to warrant investigations separate from those of choline when they are measured on a second-by-second time scale.

Finally, we sought to examine the relationships between resting levels of neurotransmitters and the KCl-evoked release of neurotransmitters. Over the course of analyzing our data, we noticed increased resting levels of glutamate with decreased KCl-evoked release of glutamate compared to ACh. The two neurotransmitters almost seemed to have an inverse relationship to each other in these two parameters. We were interested in whether the KCl-evoked release of a neurotransmitter was correlated to its resting levels, so we performed correlations for each neurotransmitter within the three subregions (Figure 7). The correlation between the log of the evoked release of ACh and resting levels of ACh in the Cg1 was found to be significant. We did not see any significant correlations in our glutamate data, nor did we find significance in the PrL and IL regions for ACh. These findings suggest that the tonic and phasic aspects of signaling in the mPFC are independent of each other. However, resting ACh levels may be predictive of KCl-evoked ACh release in the Cg1.

In conclusion, we believe that this series of studies is critical to furthering our understanding of prefrontal cortex neurochemistry. We observed no significant differences in tonic and phasic release of glutamate or ACh in subregions of the mPFC subregions. However, we did see greater amounts of resting glutamate compared to resting ACh levels in the three subregions of the mPFC. In addition, the amount of potassium-evoked ACh release was greater as compared to potassium-evoked glutamate release in all subregions of the mPFC. Finally, when the potassium-evoked signals of glutamate or ACh were expressed relative to baseline, it was found that potassium-evoked ACh release was 500-1000 % of baseline whereas glutamate was no greater than 100% of baseline, supporting that there was evidence for potential autoregulation of both neurotransmitters. The next step is to continue these recordings in awake, freely moving animals with the goal of exploring glutamate and ACh signaling in the prefrontal cortex during behavior without the potential confound of anesthesia. Also planned are experiments that use drugs such as TTX and TBOA to determine the neuronal contribution to glutamate and ACh signals in the mPFC. Additionally, while these studies used separate MEAs to measure glutamate and ACh, the development of a novel MEA design that allows for measurement of multiple chemicals of interest at the same time (Hascup et al., 2007) should prove to be very useful for determining relationships between different neurotransmitter systems *in vivo*.

Acknowledgments

This work was supported by USPHS grants DA 017186 and salary support from a training grant T32 DA016176 for Catherine Mattinson.

References

Abekawa T, Ohmori T, Ito K, Koyama T. D1 dopamine receptor activation reduces extracellular glutamate and GABA concentrations in the medial prefrontal cortex. Brain Res. 2000; 867:250–4. [PubMed: 10837822]

Arnold HM, Fadel J, Sarter M, Bruno JP. Amphetamine-stimulated cortical acetylcholine release: role of the basal forebrain. Brain Res. 2001; 894:74–87. [PubMed: 11245817]

Arnold HM, Nelson CL, Sarter M, Bruno JP. Sensitization of cortical acetylcholine release by repeated administration of nicotine in rats. Psychopharmacology (Berl). 2003; 165:346–58. [PubMed: 12454730]

Bailey KR, Mair RG. Lesions of specific and nonspecific thalamic nuclei affect prefrontal cortex-dependent aspects of spatial working memory. Behav Neurosci. 2005; 119:410–9. [PubMed: 15839787]

Bauer D, Gupta D, Harotunian V, Meador-Woodruff JH, McCullumsmith RE. Abnormal expression of glutamate transporter and transporter interacting molecules in prefrontal cortex in elderly patients with schizophrenia. Schizophr Res. 2008; 104:108–20. [PubMed: 18678470]

Benes FM, Sorensen I, Vincent SL, Bird ED, Sathi M. Increased density of glutamate-immunoreactive vertical processes in superficial laminae in cingulate cortex of schizophrenic brain. Cereb Cortex. 1992; 2:503–12. [PubMed: 1282404]

Berger B, Thierry AM, Tassin JP, Moyne MA. Dopaminergic innervation of the rat prefrontal cortex: a fluorescence histochemical study. Brain Res. 1976; 106:133–45. [PubMed: 1268702]

Bigl V, Woolf NJ, Butcher LL. Cholinergic projections from the basal forebrain to frontal, parietal, temporal, occipital, and cingulate cortices: a combined fluorescent tracer and acetylcholinesterase analysis. Brain Res Bull. 1982; 8:727–49. [PubMed: 6182962]

Brooks JM, Sarter M, Bruno JP. D2-like receptors in nucleus accumbens negatively modulate acetylcholine release in prefrontal cortex. Neuropharmacology. 2007; 53:455–63. [PubMed: 17681559]

Brown RM, Crane AM, Goldman PS. Regional distribution of monoamines in the cerebral cortex and subcortical structures of the rhesus monkey: concentrations and in vivo synthesis rates. Brain Res. 1979; 168:133–50. [PubMed: 36962]

Bruno JP, Gash C, Martin B, Zmarowski A, Pomerleau F, Burmeister J, Huettl P, Gerhardt GA. Second-by-second measurement of acetylcholine release in prefrontal cortex. Eur J Neurosci. 2006; 24:2749–57. [PubMed: 17156201]

Burbaeva G, Boksha IS, Tereshkina EB, Savushkina OK, Starodubtseva LI, Turishcheva MS. Glutamate metabolizing enzymes in prefrontal cortex of Alzheimer's disease patients. Neurochem Res. 2005; 30:1443–51. [PubMed: 16341942]

Burmeister JJ, Gerhardt GA. Self-referencing ceramic-based multisite microelectrodes for the detection and elimination of interferences from the measurement of L-glutamate and other analytes. Anal Chem. 2001; 73:1037–42. [PubMed: 11289414]

Burmeister JJ, Moxon K, Gerhardt GA. Ceramic-based multisite microelectrodes for electrochemical recordings. Anal Chem. 2000; 72:187–92. [PubMed: 10655652]

Burmeister JJ, Pomerleau F, Huettl P, Gash CR, Werner CE, Bruno JP, Gerhardt GA. Ceramic-based multisite microelectrode arrays for simultaneous measures of choline and acetylcholine in CNS. Biosens Bioelectron. 2008; 23:1382–9. [PubMed: 18243683]

Burmeister JJ, Pomerleau F, Palmer M, Day BK, Huettl P, Gerhardt GA. Improved ceramic-based multisite microelectrode for rapid measurements of L-glutamate in the CNS. J Neurosci Methods. 2002; 119:163–71. [PubMed: 12323420]

Clapp-Lilly KL, Roberts RC, Duffy LK, Irons KP, Hu Y, Drew KL. An ultrastructural analysis of tissue surrounding a microdialysis probe. J Neurosci Methods. 1999; 90:129–42. [PubMed: 10513596]

Crook JM, Tomaskovic-Crook E, Copolov DL, Dean B. Low muscarinic receptor binding in prefrontal cortex from subjects with schizophrenia: a study of Brodmann's areas 8, 9, 10, and 46 and the effects of neuroleptic drug treatment. Am J Psychiatry. 2001; 158:918–25. [PubMed: 11384900]

Danbolt NC. Glutamate uptake. Prog Neurobiol. 2001; 65:1–105. [PubMed: 11369436]

Day BK, Pomerleau F, Burmeister JJ, Huettl P, Gerhardt GA. Microelectrode array studies of basal and potassium-evoked release of L-glutamate in the anesthetized rat brain. J Neurochem. 2006; 96:1626–35. [PubMed: 16441510]

de Brabander JM, van Eden CG, de Bruin JP, Feenstra MG. Monoamine concentrations in rat prefrontal cortex and other mesolimbocortical structures in response to partial neonatal lesions of the medial prefrontal cortex. Brain Res. 1993; 601:20–7. [PubMed: 8431765]

Del Arco A, Martinez R, Mora F. Amphetamine increases extracellular concentrations of glutamate in the prefrontal cortex of the awake rat: a microdialysis study. Neurochem Res. 1998; 23:1153–8. [PubMed: 9712184]

Del Arco A, Segovia G, Garrido P, de Blas M, Mora F. Stress, prefrontal cortex and environmental enrichment: studies on dopamine and acetylcholine release and working memory performance in rats. Behav Brain Res. 2007; 176:267–73. [PubMed: 17097747]

Ferraro L, Tomasini MC, Gessa GL, Bebe BW, Tanganelli S, Antonelli T. The cannabinoid receptor agonist WIN 55,212-2 regulates glutamate transmission in rat cerebral cortex: an in vivo and in vitro study. Cereb Cortex. 2001; 11:728–33. [PubMed: 11459762]

Francis PT, Palmer AM, Snape M, Wilcock GK. The cholinergic hypothesis of Alzheimer's disease: a review of progress. J Neurol Neurosurg Psychiatry. 1999; 66:137–47. [PubMed: 10071091]

Frantz K, Harte M, Ungerstedt U, WT OC. A dual probe characterization of dialysate amino acid levels in the medial prefrontal cortex and ventral tegmental area of the awake freely moving rat. J Neurosci Methods. 2002; 119:109–19. [PubMed: 12323414]

Friedemann MN, Gerhardt GA. Regional effects of aging on dopaminergic function in the Fischer-344 rat. Neurobiol Aging. 1992; 13:325–32. [PubMed: 1522947]

Georgieva J, Luthman J, Mohringe B, Magnusson O. Tissue and microdialysate changes after repeated and permanent probe implantation in the striatum of freely moving rats. Brain Res Bull. 1993; 31:463–70. [PubMed: 8098651]

Gigg J, Tan AM, Finch DM. Glutamatergic excitatory responses of anterior cingulate neurons to stimulation of the mediodorsal thalamus and their regulation by GABA: an in vivo iontophoretic study. Cereb Cortex. 1992; 2:477–84. [PubMed: 1282403]

Gigg J, Tan AM, Finch DM. Glutamatergic hippocampal formation projections to prefrontal cortex in the rat are regulated by GABAergic inhibition and show convergence with glutamatergic projections from the limbic thalamus. Hippocampus. 1994; 4:189–98. [PubMed: 7951693]

Giuliano C, Parikh V, Ward JR, Chiamulera C, Sarter M. Increases in cholinergic neurotransmission measured by using choline-sensitive microelectrodes: enhanced detection by hydrolysis of acetylcholine on recording sites? Neurochem Int. 2008; 52:1343–50. [PubMed: 18346819]

Grabb MC, Sciotti VM, Gidday JM, Cohen SA, van Wylen DG. Neurochemical and morphological responses to acutely and chronically implanted brain microdialysis probes. J Neurosci Methods. 1998; 82:25–34. [PubMed: 10223512]

Gratton A, Hoffer BJ, Gerhardt GA. In vivo electrochemical studies of monoamine release in the medial prefrontal cortex of the rat. Neuroscience. 1989; 29:57–64. [PubMed: 2710348]

Hara K, Harris RA. The anesthetic mechanism of urethane: the effects on neurotransmitter-gated ion channels. Anesth Analg. 2002; 94:313–8. table of contents. [PubMed: 11812690]

Hascup ER, Hascup KN, Stephens M, Pomerleau F, Huettl P, Gratton A, Gerhardt GA. Rapid microelectrode measurements and the origin and regulation of extracellular glutamate in rat prefrontal cortex. J Neurochem. 2010; 115:1608–20. [PubMed: 20969570]

Hascup KN, Rutherford EC, Quintero JE, Day BK, Nickell JR, Pomerleau F, Huettl P, Burmeister JJ, Gerhardt GA. Second-by-Second Measures of L-Glutamate and Other Neurotransmitters Using Enzyme-Based Microelectrode Arrays. 2007

Hedou G, Homberg J, Martin S, Wirth K, Feldon J, Heidbreder CA. Effect of amphetamine on extracellular acetylcholine and monoamine levels in subterritories of the rat medial prefrontal cortex. Eur J Pharmacol. 2000; 390:127–36. [PubMed: 10708716]

Henny P, Jones BE. Projections from basal forebrain to prefrontal cortex comprise cholinergic, GABAergic and glutamatergic inputs to pyramidal cells or interneurons. Eur J Neurosci. 2008; 27:654–70. [PubMed: 18279318]

Hernandez LF, Segovia G, Mora F. Chronic treatment with a dopamine uptake blocker changes dopamine and acetylcholine but not glutamate and GABA concentrations in prefrontal cortex, striatum and nucleus accumbens of the awake rat. Neurochem Int. 2008; 52:457–69. [PubMed: 17881090]

Herzog CD, Nowak KA, Sarter M, Bruno JP. Microdialysis without acetylcholinesterase inhibition reveals an age-related attenuation in stimulated cortical acetylcholine release. Neurobiol Aging. 2003; 24:861–3. [PubMed: 12927768]

Houser CR, Crawford GD, Salvaterra PM, Vaughn JE. Immunocytochemical localization of choline acetyltransferase in rat cerebral cortex: a study of cholinergic neurons and synapses. J Comp Neurol. 1985; 234:17–34. [PubMed: 3980786]

Huang M, Li Z, Dai J, Shahid M, Wong EH, Meltzer HY. Asenapine increases dopamine, norepinephrine, and acetylcholine efflux in the rat medial prefrontal cortex and hippocampus. Neuropsychopharmacology. 2008; 33:2934–45. [PubMed: 18418367]

Hugues S, Garcia R, Lena I. Time course of extracellular catecholamine and glutamate levels in the rat medial prefrontal cortex during and after extinction of conditioned fear. Synapse. 2007; 61:933–7. [PubMed: 17663454]

Jay TM, Thierry AM, Wiklund L, Glowinski J. Excitatory Amino Acid Pathway from the Hippocampus to the Prefrontal Cortex. Contribution of AMPA Receptors in Hippocampo-prefrontal Cortex Transmission. Eur J Neurosci. 1992; 4:1285–95. [PubMed: 12106392]

Karreman M, Moghaddam B. Effect of a pharmacological stressor on glutamate efflux in the prefrontal cortex. Brain Res. 1996; 716:180–2. [PubMed: 8738235]

Kashani A, Lepicard E, Poirel O, Videau C, David JP, Fallet-Bianco C, Simon A, Delacourte A, Giros B, Epelbaum J, Betancur C, El Mestikawy S. Loss of VGLUT1 and VGLUT2 in the prefrontal cortex is correlated with cognitive decline in Alzheimer disease. Neurobiol Aging. 2008; 29:1619–30. [PubMed: 17531353]

Lawler HC. Turnover time of acetylcholinesterase. J Biol Chem. 1961; 236:2296–301. [PubMed: 13759667]

Leonard CM. The prefrontal cortex of the rat. I. Cortical projection of the mediodorsal nucleus. II. Efferent connections. Brain Res. 1969; 12:321–43. [PubMed: 4184997]

Lu W, Monteggia LM, Wolf ME. Withdrawal from repeated amphetamine administration reduces NMDAR1 expression in the rat substantia nigra, nucleus accumbens and medial prefrontal cortex. Eur J Neurosci. 1999; 11:3167–77. [PubMed: 10510180]

Lupinsky D, Moquin L, Gratton A. Interhemispheric regulation of the medial prefrontal cortical glutamate stress response in rats. J Neurosci. 2010; 30:7624–33. [PubMed: 20519537]

McDonald AJ. Glutamate and aspartate immunoreactive neurons of the rat basolateral amygdala: colocalization of excitatory amino acids and projections to the limbic circuit. J Comp Neurol. 1996; 365:367–79. [PubMed: 8822176]

McFarland K, Lapish CC, Kalivas PW. Prefrontal glutamate release into the core of the nucleus accumbens mediates cocaine-induced reinstatement of drug-seeking behavior. J Neurosci. 2003; 23:3531–7. [PubMed: 12716962]

McGaughy J, Kaiser T, Sarter M. Behavioral vigilance following infusions of 192 IgG-saporin into the basal forebrain: selectivity of the behavioral impairment and relation to cortical AChE-positive fiber density. Behav Neurosci. 1996; 110:247–65. [PubMed: 8731052]

Mesulam MM, Mufson EJ, Wainer BH, Levey AI. Central cholinergic pathways in the rat: an overview based on an alternative nomenclature (Ch1-Ch6). Neuroscience. 1983; 10:1185–201. [PubMed: 6320048]

Meyer EM Jr, Engel DA, Cooper JR. Acetylation and phosphorylation of choline following high or low affinity uptake by rat cortical synaptosomes. Neurochem Res. 1982; 7:749–59. [PubMed: 7121721]

Miele M, Berners M, Boutelle MG, Kusakabe H, Fillenz M. The determination of the extracellular concentration of brain glutamate using quantitative microdialysis. Brain Res. 1996; 707:131–3. [PubMed: 8866723]

Mork A, Witten LM, Arnt J. Effect of sertindole on extracellular dopamine, acetylcholine, and glutamate in the medial prefrontal cortex of conscious rats: a comparison with risperidone and

exploration of mechanisms involved. Psychopharmacology (Berl). 2009; 206:39–49. [PubMed: 19506838]

Mrzljak L, Goldman-Rakic PS. Acetylcholinesterase reactivity in the frontal cortex of human and monkey: contribution of AChE-rich pyramidal neurons. J Comp Neurol. 1992; 324:261–81. [PubMed: 1430332]

Nandi P, Lunte SM. Recent trends in microdialysis sampling integrated with conventional and microanalytical systems for monitoring biological events: a review. Anal Chim Acta. 2009; 651:1–14. [PubMed: 19733728]

Neigh-McCandless G, Kravitz BA, Sarter M, Bruno JP. Stimulation of cortical acetylcholine release following blockade of ionotropic glutamate receptors in nucleus accumbens. Eur J Neurosci. 2002; 16:1259–66. [PubMed: 12405986]

Nickell J, Pomerleau F, Allen J, Gerhardt GA. Age-related changes in the dynamics of potassium-evoked L-glutamate release in the striatum of Fischer 344 rats. J Neural Transm. 2005; 112:87–96. [PubMed: 15599607]

Nirogi R, Mudigonda K, Kandikere V, Ponnamaneni R. Quantification of acetylcholine, an essential neurotransmitter, in brain microdialysis samples by liquid chromatography mass spectrometry. Biomed Chromatogr. 2010; 24:39–48. [PubMed: 19877295]

Okuda T, Haga T, Kanai Y, Endou H, Ishihara T, Katsura I. Identification and characterization of the high-affinity choline transporter. Nat Neurosci. 2000; 3:120–5. [PubMed: 10649566]

Olbrich HM, Valerius G, Rusch N, Buchert M, Thiel T, Hennig J, Ebert D, Van Elst LT. Frontolimbic glutamate alterations in first episode schizophrenia: evidence from a magnetic resonance spectroscopy study. World J Biol Psychiatry. 2008; 9:59–63. [PubMed: 17853298]

Oni-Orisan A, Kristiansen LV, Haroutunian V, Meador-Woodruff JH, McCullumsmith RE. Altered vesicular glutamate transporter expression in the anterior cingulate cortex in schizophrenia. Biol Psychiatry. 2008; 63:766–75. [PubMed: 18155679]

Paxinos, G.; Watson, C. The Rat Brain in Stereotaxic Coordinates. Fifth. Academic Press; San Diego, CA: 2004.

Perry JL, Joseph JE, Jiang Y, Zimmerman RS, Kelly TH, Darna M, Huettl P, Dwoskin LP, Bardo MT. Prefrontal cortex and drug abuse vulnerability: translation to prevention and treatment interventions. Brain Res Rev. 2011; 65:124–49. [PubMed: 20837060]

Pirot S, Jay TM, Glowinski J, Thierry AM. Anatomical and electrophysiological evidence for an excitatory amino acid pathway from the thalamic mediodorsal nucleus to the prefrontal cortex in the rat. Eur J Neurosci. 1994; 6:1225–34. [PubMed: 7524967]

Prus AJ, Huang M, Li Z, Dai J, Meltzer HY. The neurotensin analog NT69L enhances medial prefrontal cortical dopamine and acetylcholine efflux: potentiation of risperidone-, but not haloperidol-, induced dopamine efflux. Brain Res. 2007; 1184:354–64. [PubMed: 17988654]

Ragozzino ME, Unick KE, Gold PE. Hippocampal acetylcholine release during memory testing in rats: augmentation by glucose. Proc Natl Acad Sci U S A. 1996; 93:4693–8. [PubMed: 8643466]

Rajkowska G, Niewiadomska G, Kosmal A. Regional and laminar variations in acetylcholinesterase activity within the frontal cortex of the dog. J Chem Neuroanat. 1993; 6:117–30. [PubMed: 7688230]

Romanides AJ, Duffy P, Kalivas PW. Glutamatergic and dopaminergic afferents to the prefrontal cortex regulate spatial working memory in rats. Neuroscience. 1999; 92:97–106. [PubMed: 10392833]

Rutherford EC, Pomerleau F, Huettl P, Stromberg I, Gerhardt GA. Chronic second-by-second measures of L-glutamate in the central nervous system of freely moving rats. J Neurochem. 2007; 102:712–22. [PubMed: 17630982]

Sarter M, Nelson CL, Bruno JP. Cortical cholinergic transmission and cortical information processing in schizophrenia. Schizophr Bull. 2005; 31:117–38. [PubMed: 15888431]

Schultz KN, Kennedy RT. Time-resolved microdialysis for in vivo neurochemical measurements and other applications. Annu Rev Anal Chem (Palo Alto Calif). 2008; 1:627–61. [PubMed: 20636092]

Selim M, Bradberry CW. Effect of ethanol on extracellular 5-HT and glutamate in the nucleus accumbens and prefrontal cortex: comparison between the Lewis and Fischer 344 rat strains. Brain Res. 1996; 716:157–64. [PubMed: 8738232]

Sofuoglu M, Mooney M. Cholinergic functioning in stimulant addiction: implications for medications development. CNS Drugs. 2009; 23:939–52. [PubMed: 19845415]

Stephens ML, Quintero JE, Pomerleau F, Huettl P, Gerhardt GA. Age-related changes in glutamate release in the CA3 and dentate gyrus of the rat hippocampus. Neurobiol Aging. 2009

Thierry AM, Deniau JM, Chevalier G, Ferron A, Glowinski J. An electrophysiological analysis of some afferent and efferent pathways of the rat prefrontal cortex. Prog Brain Res. 1983; 58:257–61. [PubMed: 6415755]

Timmerman W, Westerink BH. Brain microdialysis of GABA and glutamate: what does it signify? Synapse. 1997; 27:242–61. [PubMed: 9329159]

Torres EM, Perry TA, Blockland A, Wilkinson LS, Wiley RG, Lappi DA, Dunnet SB. Behavioural, histochemical and biochemical consequences of selective immunolesions in discrete regions of the basal forebrain cholinergic system. Neuroscience. 1994; 63:95–122. [PubMed: 7898665]

Trabace L, Cassano T, Colaianna M, Castrignano S, Giustino A, Amoroso S, Steardo L, Cuomo V. Neurochemical and neurobehavioral effects of ganstigmine (CHF2819), a novel acetylcholinesterase inhibitor, in rat prefrontal cortex: an in vivo study. Pharmacol Res. 2007; 56:288–94. [PubMed: 17822918]

Tsai G, Passani LA, Slusher BS, Carter R, Baer L, Kleinman JE, Coyle JT. Abnormal excitatory neurotransmitter metabolism in schizophrenic brains. Arch Gen Psychiatry. 1995; 52:829–36. [PubMed: 7575102]

Welty N, Shoblock JR. The effects of thioperamide on extracellular levels of glutamate and GABA in the rat prefrontal cortex. Psychopharmacology (Berl). 2009; 207:433–8. [PubMed: 19795107]

Williams JM, Steketee JD. Cocaine increases medial prefrontal cortical glutamate overflow in cocaine-sensitized rats: a time course study. Eur J Neurosci. 2004; 20:1639–46. [PubMed: 15355331]

Woo TU, Kim AM, Viscidi E. Disease-specific alterations in glutamatergic neurotransmission on inhibitory interneurons in the prefrontal cortex in schizophrenia. Brain Res. 2008; 1218:267–77. [PubMed: 18534564]

Zmarowski A, Wu HQ, Brooks JM, Potter MC, Pellicciari R, Schwarcz R, Bruno JP. Astrocyte-derived kynurenic acid modulates basal and evoked cortical acetylcholine release. Eur J Neurosci. 2009; 29:529–38. [PubMed: 19187269]

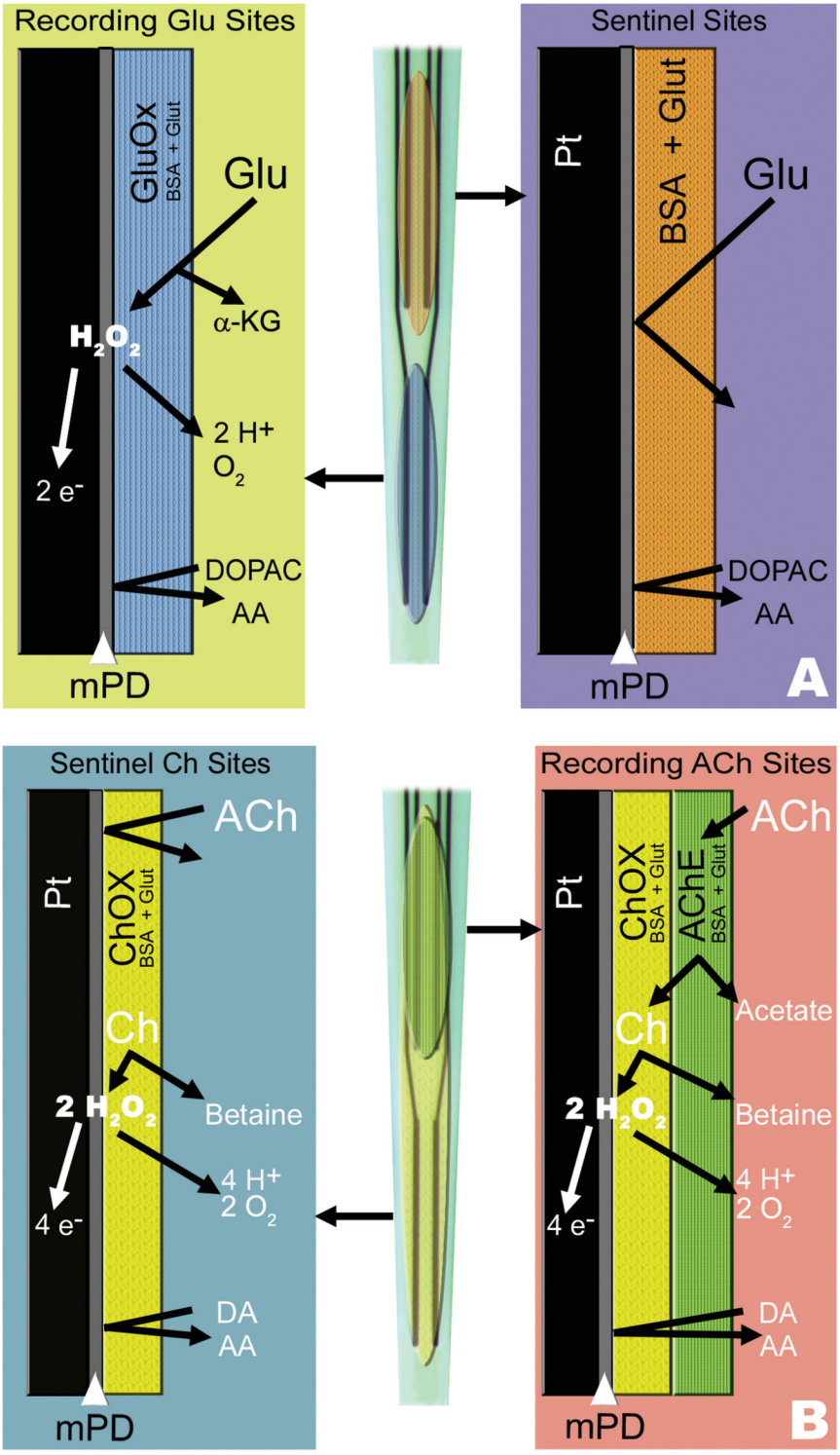

Fig. 1.

Configurations of surface coatings for measures of tonic and phasic release of glutamate or ACh. A) One pair of recordings sites on the MEAS is coated with glutamate oxidase (GluOx) and an inert BSA and glutaraldehyde coating for glutamate detection. Glutamate comes into contact with the GluOx layer and is oxidized into H_2O_2 and α-ketoglutarate.

When the H_2O_2 comes into contact with the Pt recording sites the H_2O_2 is oxidized and the resulting electrons generated are proportional to the concentration of glutamate. An mPD exclusion layer serves to block potential electroactive interferents such as ascorbic acid (AA). The signal detected at the sentinel sites is subtracted from the glutamate signal generating a self-referenced glutamate signal and resultant glutamate resting level measurement. B) For the detection of ACh, one pair of sites is coated with human recombinant acetylcholinesterase (AChE) and choline oxidase (ChOx), while the other is coated with only ChOx. When ACh comes into contact with the enzyme layers, AChE hydrolyzes ACh into choline and acetate. The choline is in turn oxidized by the ChOx into H_2O_2 and betaine. Similar to the glutamate MEA, the H_2O_2 is oxidized at the Pt site producing a signal current that is directly proportional to the concentration of choline. mPD is used to exclude electroactive interferents such as AA. The sentinel ChOx coated sites generate a choline signal, which is subtracted from the combined ACh/choline signal, resulting in a self-referenced ACh signal for measures of ACh resting levels.

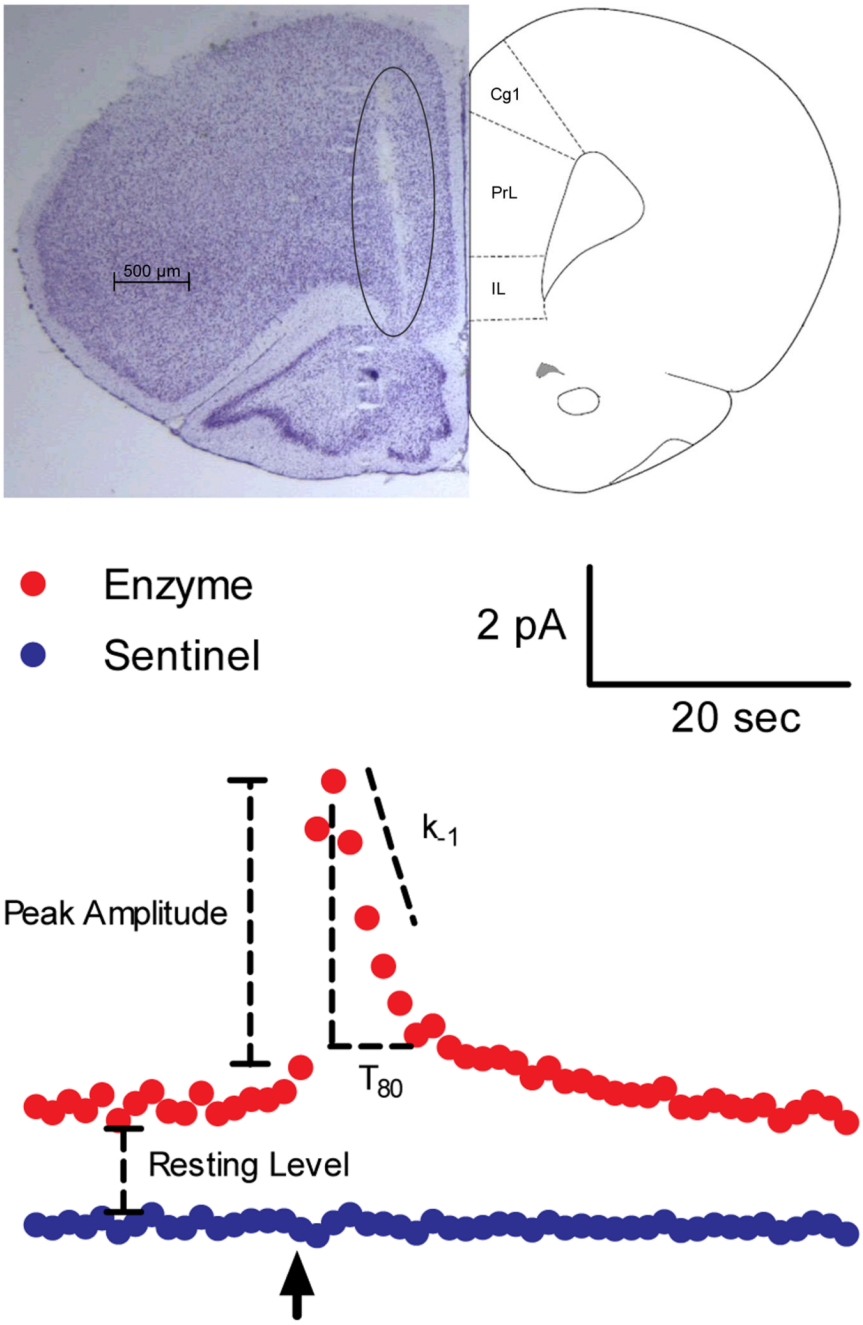

Fig. 2.

A) Histological section with cresyl violet staining showing minimal damage produced by the MEA. Histological sections were used to confirm placement in the mPFC Cg1, PrL, and IL. B) Raw current signals from active (upper trace) and sentinel MEA recording sites (lower trace) showing a typical recording of resting and potassium-evoked release of glutamate or ACh. *In vivo* ejection of KCl produces a rapid increase in glutamate or ACh that quickly clears to baseline on the enzyme-coated channel, while the sentinel channel does not show a response. This allows for sentinel channel subtraction to obtain a self-referenced signal that is the resting level of the neurotransmitter. Parameters used in data analysis include resting levels, peak amplitudes, T_{80} values, and the k_{-1} first-order rate constant.

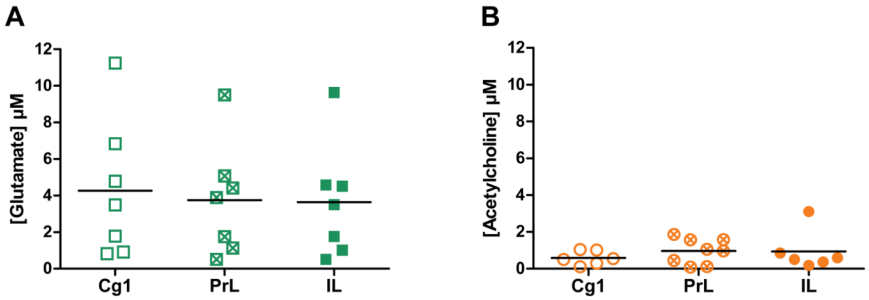

Fig. 3.

Resting or tonic levels of glutamate and ACh in subregions of the mPFC A) Resting levels of glutamate were homogeneous and not significantly different within subregions of the mPFC. (n = 7 for all regions). B) Resting levels of ACh were not significantly different within subregions of the mPFC (Cg1 and IL, n = 6; PrL, n = 8).

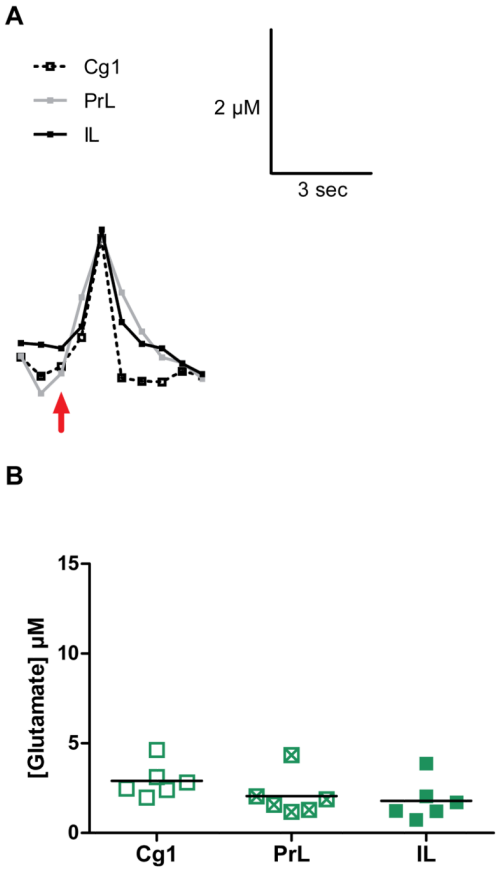

Fig. 4.

KCl-evoked glutamate release in the mPFC. A) Shown are representative signals from the Cg1, PrL and IL of the mPFC. The arrow marks the ejection of KCl to evoke phasic release of glutamate. B) Graphs showing the maximum amplitudes of KCl-evoked release in the different subregions of the mPFC. The average amplitudes of KCl-evoked glutamate release were not significantly different in the three brain regions.

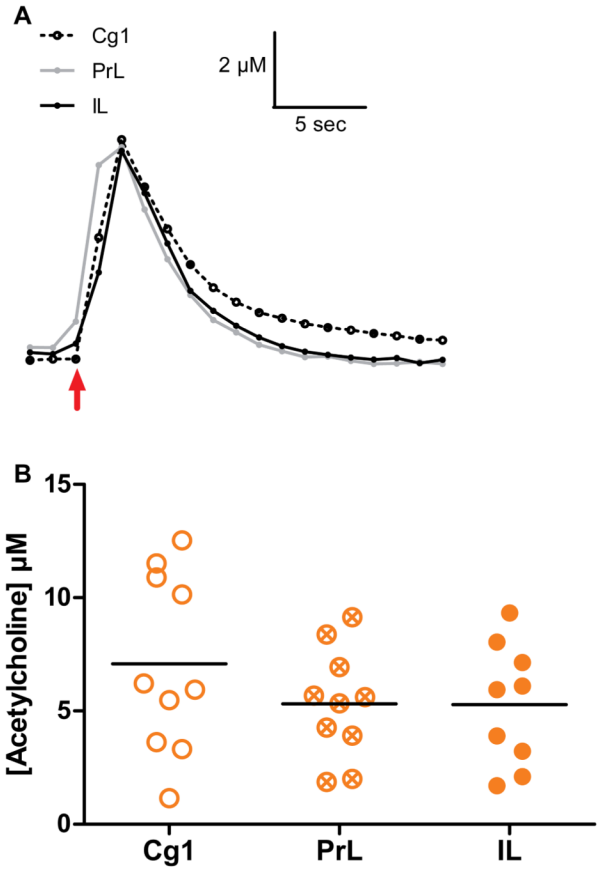

Fig. 5.

KCl-evoked ACh release in subregions of the mPFC. A) Shown are single traces of KCl-evoked ACh release from the Cg1, PrL and IL of the mPFC. The arrow marks the ejection of KCl to evoke phasic release of Ach. B) Graphs showing average amplitudes of KCl-evoked ACh release in the 3 subregions of the mPFC. There was no significant difference in the ACh amplitudes within the different subregions along the dorsal-ventral axis of the mPFC. (Cg1 and PrL, n = 10; IL, n = 9).

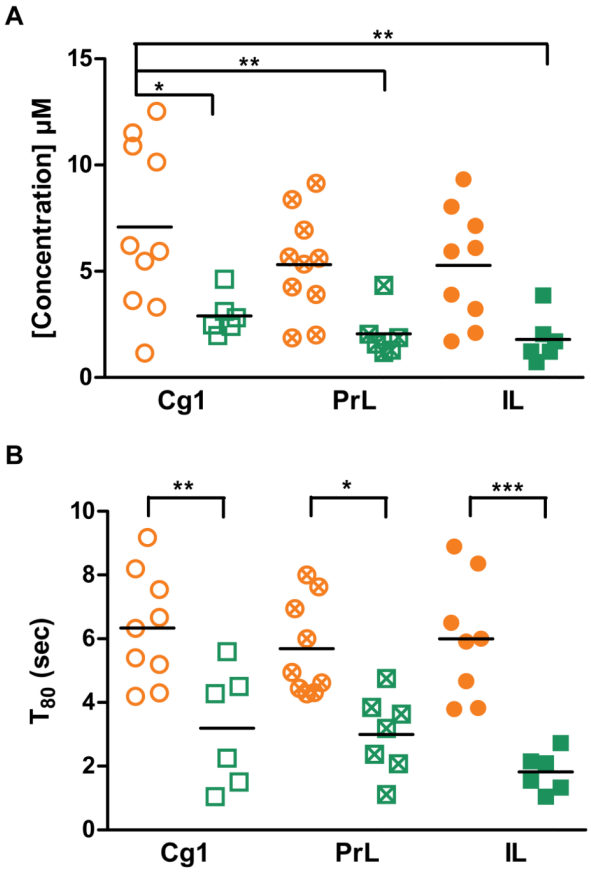

Fig. 6.

Comparison of glutamate and ACh peak amplitudes and T_{80} values in different subregions of the mPFC. A) Significant differences were found between the potassium-evoked ACh signal amplitudes (orange circles) in the Cg1 (**p < 0.01; *p < 0.05; Glu: n = 6; ACh: Cg1 and PrL, n = 10, IL, n = 9) as compared to glutamate signaling (green squares) in the three subregions of the mPFC. B) T80 values differ significantly between glutamate and ACh in each subregion (***p < 0.001; **p < 0.01; *p < 0.05; Glu: Cg1 and IL, n = 6, PrL, n = 7; ACh: Cg1 and PrL, n = 9, IL, n = 8).

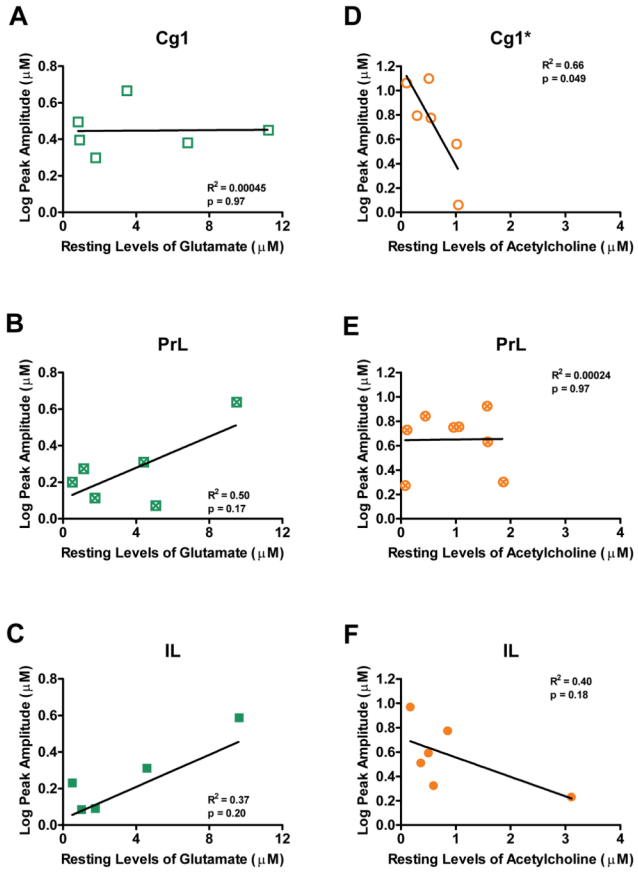

Fig. 7.

Correlations of glutamate and ACh peak amplitudes and resting levels. A, B, C) The correlations of the log of KCl-evoked glutamate peak amplitudes and glutamate resting levels were not significant (Cg1 and PrL, n = 5; IL, n = 5). D, E, F) The log of KCl-evoked ACh peak amplitudes and ACh resting levels showed a significant correlation in the Cg1 subregion of the mPFC ($p < 0.05$). Other subregions did not show any significant correlations (Cg1 and IL, n = 6; PrL, n = 8).

Table I

KCl-evoked glutamate release data

Subregion	Peak Amplitude	T_{80} Value	k_{-1}
Cg1	2.9 ± 0.9 μM	3.2 ± 1.8 s	0.7 ± 0.7 s^{-1}
PrL	2.0 ± 1.1 μM	3.0 ± 1.2 s	0.6 ± 0.9 s^{-1}
IL	1.8 ± 1.1 μM	1.8 ± 0.6 s	0.8 ± 0.9 s^{-1}

Glutamate signal values from subregions of the mPFC. Peak amplitudes, T_{80} values, and k_{-1} values for each of the three subregions highlight the homogeneity of the mPFC (mean ± SD; Cg1 and IL: n = 6; PrL: peak amplitude, n = 6, T_{80} value and k_{-1}, n = 7).

Table II

KCl-evoked acetylcholine release data

Subregion	Peak Amplitude	T_{80} Value	k_{-1}
Cg1	7.1 ± 3.9 μM	6.3 ± 1.7 s	0.3 ± 0.4 s^{-1}
PrL	5.3 ± 2.4 μM	5.7 ± 1.5 s	0.3 ± 0.3 s^{-1}
IL	5.3 ± 2.7 μM	6.0 ± 1.9 s	0.3 ± 0.3 s^{-1}

Acetylcholine signal parameters from subregions of the mPFC. Peak amplitudes, T80 values, and k_{-1} values for each of the three subregions highlight the homogeneity of the mPFC, and ACh release data (mean ± SD; Cg1 and PrL: peak amplitude and k_{-1}, n = 10, T_{80} value, n = 9; IL: peak amplitude, and k_{-1}, n = 9, T_{80}, n = 8).